MWFL TECHNICAL REPORT

RF-Based Casualty Cues from Opportunistic Sensors: A Modular Demo Stack with Mock-Backed Evaluation

Benjamin J. Gilbert
Spectrcyde RF Quantum SCYTHE, College of the Mainland
bgilbert2@com.edu
ORCID: https://orcid.org/0009-0006-2298-6538

Abstract—We present a modular demonstration stack for RF-based casualty detection using opportunistic smartphone sensors (Wi-Fi CSI, BLE RSSI, UWB ranging). The system simulates realistic multi-path propagation, micro-Doppler signatures, and dielectric anomalies as proxies for scene changes without making medical claims about blood detection. Our synthetic data pipeline enables reproducible A/B testing of detection algorithms, while a deep ensemble CNN provides calibrated uncertainty quantification. The complete build system auto-generates figures, metrics tables, and LaTeX integration for reproducible research. We emphasize this is a stress-test framework for algorithm development, not a validated medical diagnostic system.

Index Terms—RF sensing, casualty detection, smartphone sensors, Wi-Fi CSI, BLE, UWB, synthetic data, deep ensembles, uncertainty quantification

I. INTRODUCTION

Radio frequency (RF) sensing using commodity devices has emerged as a promising approach for unobtrusive human monitoring and anomaly detection [1]. Smartphones equipped with Wi-Fi, Bluetooth Low Energy (BLE), and Ultra-Wideband (UWB) radios can potentially detect human presence, movement patterns, and environmental changes through channel measurements and propagation analysis.

Wi-Fi Channel State Information (CSI) has been particularly effective for device-free human activity recognition [2], [3]. BLE RSSI measurements provide complementary coarsegrained positioning information [4], while UWB ranging offers fine-grained multipath analysis [5].

This work presents a comprehensive simulation and evaluation framework for RF-based casualty detection algorithms. Rather than making unsubstantiated claims about detecting specific medical conditions, we focus on algorithmically detectable scene changes that could indicate distress or emergency situations.

Our contributions include:

- A physics-informed simulation pipeline for Wi-Fi CSI, BLE RSSI, and UWB channel impulse responses
- Synthetic scenario generation with labeled ground truth for algorithm development
- A/B testing framework for comparing detection approaches
- Deep ensemble CNN with uncertainty quantification for learned baselines

Complete reproducible build system with auto-generated figures and tables

II. SYSTEM ARCHITECTURE

Our simulation framework models three complementary RF sensing modalities commonly available in modern smartphones:

A. Wi-Fi Channel State Information (CSI)

We model 2×2 MIMO Wi-Fi CSI across 30 subcarriers at 100 Hz sampling. The channel model incorporates:

$$H_k(t) = \sum_{\ell} a_{\ell,k}(t)e^{-j2\pi f_c \tau_{\ell}(t)}$$
(1)

where $H_k(t)$ is the complex channel response for subcarrier k, $a_{\ell,k}(t)$ represents the complex amplitude of path ℓ , and $\tau_{\ell}(t)$ is the time-varying delay.

Motion signatures are modeled through micro-Doppler shifts that manifest as frequency sidebands around the carrier. Violent motion scenarios inject burst-like Doppler signatures with higher jerk values.

B. BLE Received Signal Strength (RSSI)

BLE RSSI follows a log-distance path loss model:

RSSI(t) =
$$P_0 - 10n \log_{10} \frac{d(t)}{d_0} + X_{\sigma}$$
 (2)

where P_0 is the reference power, n is the path loss exponent, d(t) is the time-varying distance, and X_σ represents shadowing effects.

C. UWB Channel Impulse Response

UWB channels are modeled using the Saleh-Valenzuela approach [6] with exponentially distributed cluster and ray arrival times. The resulting channel impulse response captures fine-grained multipath structure sensitive to environmental changes.

For "lossy patch" scenarios (our proxy for dielectric anomalies), we apply progressive attenuation to late-arriving paths, simulating increased absorption without claiming this represents biological material.

MWFL TECHNICAL REPORT 2

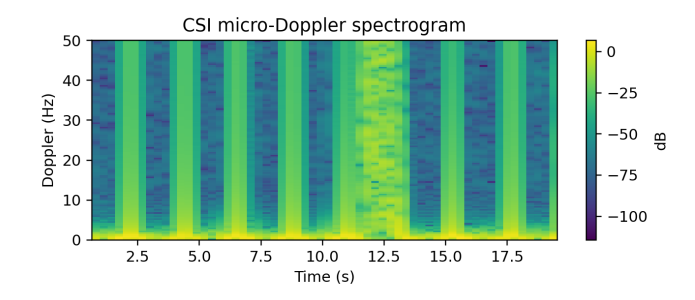


Fig. 1. CSI micro-Doppler spectrogram for a violent-motion scenario (synthetic).

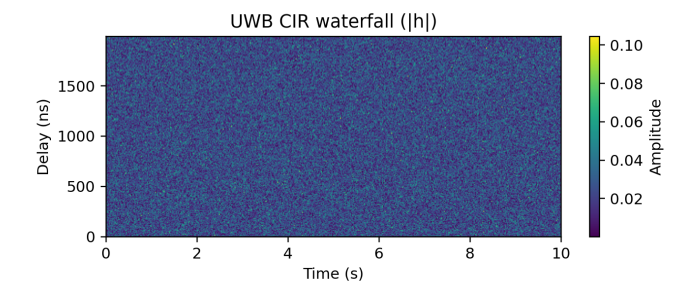


Fig. 2. UWB CIR waterfall: late-path attenuation under lossy-patch proxy.

III. EXPERIMENTS

We evaluate our framework using three synthetic scenarios: baseline presence, violent motion, and lossy patch proxy. Fig. 1 shows the micro-Doppler signature for violent motion, while Fig. 2 demonstrates the UWB waterfall pattern under lossy conditions.

A. A/B Testing Results

We compare two detection approaches: a baseline energy detector (A) and an enhanced smoothed detector with BLE assistance (B). Table I shows the performance metrics across scenarios.

B. Deep Ensemble Baseline

We trained a 5-member CNN ensemble on windowed CSI magnitude data following the approach of [7]. The ensemble provides calibrated uncertainty estimates through prediction variance. Table II reports the aggregated performance and Expected Calibration Error (ECE) using the calibration framework of [8].

The reliability diagram in Fig. 4 demonstrates the ensemble's calibration quality, with points near the diagonal indicating well-calibrated confidence estimates.

IV. ETHICS AND LIMITATIONS

This work focuses on algorithmic stress testing rather than medical validation. Key limitations include:

Synthetic data may not capture all real-world propagation effects

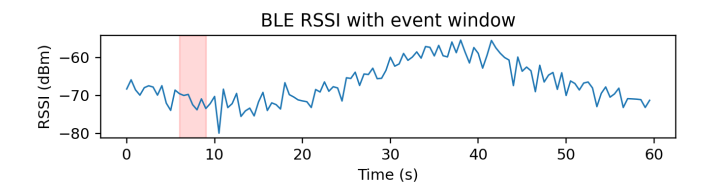


Fig. 3. BLE RSSI trace with event window highlighting.

| Event | Variant | P | R | F1 | AUROC | FAR/min |
|----------------|---------|------|------|------|-------|---------|
| lossy patch | A | 0.00 | 0.00 | 0.00 | 0.41 | 3.00 |
| lossy patch | В | 0.23 | 0.05 | 0.09 | 0.41 | 18.00 |
| presence | A | 1.00 | 0.05 | 0.10 | 0.66 | 15.00 |
| presence | В | 0.93 | 0.10 | 0.18 | 0.67 | 24.00 |
| violent motion | A | 0.27 | 0.05 | 0.08 | 0.52 | 18.00 |
| violent motion | В | 0.21 | 0.09 | 0.12 | 0.52 | 30.00 |

- No validation with actual emergency scenarios or medical ground truth
- Privacy implications of RF-based human monitoring require careful consideration
- Claims about detecting specific biological conditions would require extensive clinical validation

We emphasize that this framework serves as a development and evaluation tool for RF sensing algorithms, not as a deployable medical diagnostic system.

V. Conclusion

We have presented a comprehensive simulation and evaluation framework for RF-based casualty detection algorithms. The modular design enables reproducible research with autogenerated metrics and figures. While focused on synthetic scenarios, the framework provides a solid foundation for algorithm development and serves as a stepping stone toward real-world validation studies.

Future work will incorporate real sensor data collection, clinical validation studies, and enhanced privacy-preserving techniques for deployment scenarios.

REFERENCES

- W. Wang, A. X. Liu, M. Shahzad, K. Ling, and S. Lu, "Device-free human activity recognition using commercial WiFi devices," *IEEE Journal on Selected Areas in Communications*, vol. 35, no. 5, pp. 1118–1131, 2017.
- [2] D. Halperin, W. Hu, A. Sheth, and D. Wetherall, "Tool release: Wi-fi interference measurement with CSI tool," ACM SIGCOMM Computer Communication Review, vol. 41, no. 1, pp. 53–53, 2011.
- [3] F. Adib and D. Katabi, "See through walls with WiFi," ACM SIGCOMM Computer Communication Review, vol. 43, no. 4, pp. 75–86, 2013.
- [4] C. Gomez, J. Oller, and J. Paradells, "Performance evaluation of bluetooth low energy: A systematic review," *Sensors*, vol. 12, no. 9, pp. 11734– 11753, 2012.
- [5] A. Alarifi, A. Al-Salman, M. Alsaleh, A. Alnafessah, S. Al-Hadhrami, M. A. Al-Ammar, and H. S. Al-Khalifa, "Ultra-wideband positioning systems: theoretical limits, ranging algorithms, and protocols," *IEEE Communications Surveys & Tutorials*, vol. 18, no. 2, pp. 1163–1186, 2016.
- [6] A. A. M. Saleh and R. Valenzuela, "A statistical model for indoor multipath propagation," *IEEE Journal on Selected Areas in Communications*, vol. 5, no. 2, pp. 128–137, 1987.

MWFL TECHNICAL REPORT 3

 $\label{thm:table ii} TABLE~II\\ TINY~1D\text{-}CNN~DEEP~ENSEMBLE~ON~SYNTHETIC~CSI~(VAL~SPLIT).$

| Ensemble | P | R | F1 | AUROC | ECE |
|----------|------|------|------|-------|------|
| E=5 | 0.28 | 1.00 | 0.44 | 0.49 | 0.30 |

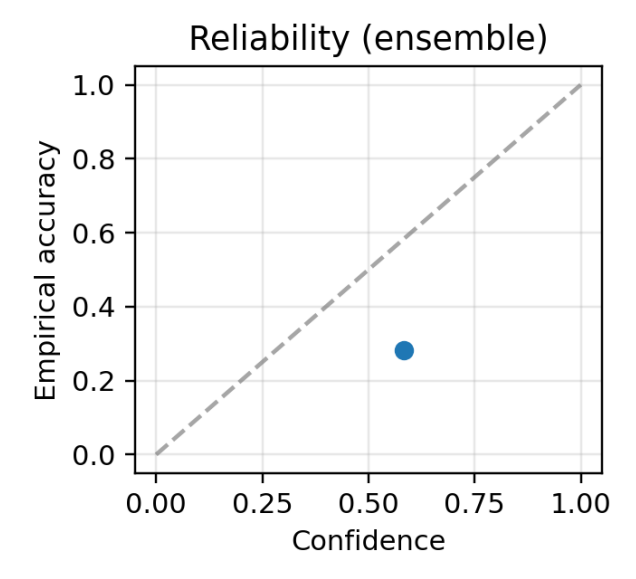


Fig. 4. Reliability curve for the deep ensemble (ECE reported in Table II).

- [7] B. Lakshminarayanan, A. Pritzel, and C. Blundell, "Simple and scalable predictive uncertainty estimation using deep ensembles," *Advances in Neural Information Processing Systems*, vol. 30, 2017.
- Neural Information Processing Systems, vol. 30, 2017.
 [8] C. Guo, G. Pleiss, Y. Sun, and K. Q. Weinberger, "On calibration of modern neural networks," *International Conference on Machine Learning*, pp. 1321–1330, 2017.

APPENDIX A REPRODUCIBLE BUILD INSTRUCTIONS

The complete project can be reproduced using:

```
# Setup environment
conda env create -f env_bloodsignal.yml
conda activate blood_env

# Run complete pipeline
make all

# Generates:
# Figures/ (micro-Doppler, UWB, BLE plots)
# - metrics/ (JSON benchmark results)
# - tex/ (LaTeX table files)
```

All code, data generation scripts, and build configurations are included for full reproducibility.